Experimental report

12/02/2019

Proposal:	**6-06-463**	**Council:**	4/2015
Title:	Local structure of uniaxial ferroelectric relaxor (Sr,Ba)Nb2O6		
Research area:	Physics		

This proposal is a resubmission of 6-06-461

Main proposer:	**Marek PASCIAK**
Experimental team:	Petr ONDREJKOVIC Marek PASCIAK Jiri KULDA
Local contacts:	Gabriel Julio CUELLO Henry FISCHER

Samples:	(Sr0.35Ba0.65)Nb2O6 (Sr0.5Ba0.5)Nb2O6 (Sr0.61Ba0.39)Nb2O6 (Sr0.86Ba0.14)Nb2O6 (Sr0.75Ba0.25)Nb2O6

Instrument	Requested days	Allocated days	From	To
D4	5	5	19/10/2015	25/10/2015

Abstract:

We propose to investigate the local structure of uniaxial relaxor ferroelectric compound (Sr,Ba)Nb2O6 using pair distribution function analysis. Knowing that the substitutional disorder has an influence on the dielectric permittivity of this compound, we plan to conduct experiments with varying Sr concentration and temperature. This study will help to better understand origin of ferroelectricity as well as an impact of Sr concetration on relaxor properties in (Sr,Ba)Nb2O6.

Local structure of relaxor ferroelectric $Sr_xBa_{1-x}Nb_2O_6$ (SBN) from pair distribution function analysis (experiment 6-06-463)

Abstract

In this work we contribute to the atomistic description of SBN by studying local structural phenomena in three compositions ($x = 0.35$, 0.5, and 0.61) over a wide temperature range. As an experimental probe we use the neutron pair distribution function (PDF) method that has proven fruitful in the understanding of short-range polar order in perovskite ferroelectric relaxors and in Pb(Zr,Ti)O_3. The experiment is complemented with *ab initio* calculations that allow us to understand the observed PDF profiles and in addition provide insights into local structural features that do not leave any strong signatures in PDF. Moreover, finite-temperature first principles molecular dynamics allows us to calculate time averages and to subtract signal broadening by phonons. In this way we can reveal a nanoscale structural change in SBN with temperature. We concentrate on three main aspects of the SBN's local structure: substitutional disorder (including vacancies), octahedra tilting and polarization and discuss how their interplay can result in SBN's unique properties.

1 Experiment

The neutron scattering experiment 6-06-463 [1] was carried out on the D4c hot neutron two-axis diffractometer. The instrument was operated in its standard configuration, using the horizontally flat Cu(220) monochromator (neutron wavelength of $\lambda = 0.5$ Å) and the Rh filter to avoid the $\lambda/2$ harmonic contamination. The 2θ-range of measured diffractograms was $1.5° - 140°$, giving a momentum-transfer range $Q \in (0.3 - 23.5)$ Å^{-1}.

A standard sealed cylindrical vanadium container of inner diameter of 6.8 mm was used as a sample holder. The powder-filled part of the container had a height of about 6 cm. Diffraction measurements were performed in both a cryostat and a furnace to cover the temperature range of $20 - 600$ K. For the sake of subtracting background intensity, diffraction patterns of the empty furnace, the empty cryostat, as well as for the empty container within both sample environments, were measured. Neutron powder diffractograms $I(Q)$ were calculated by the *d4creg* program. The resulting intensity $I(Q)$ was corrected for background intensity of the empty container and for the Placzek inelastic-scattering effect. Subsequently, the pair-distribution function (PDF) was calculated using the *d4fou* program. Here, we assumed for simplicity that the scattering intensity $I(Q)$ is proportional to $S(Q)$ without making additional corrections for, e.g. absorption, multiple scattering, other inelastic scattering beyond the Placzek correction and the sample shape.

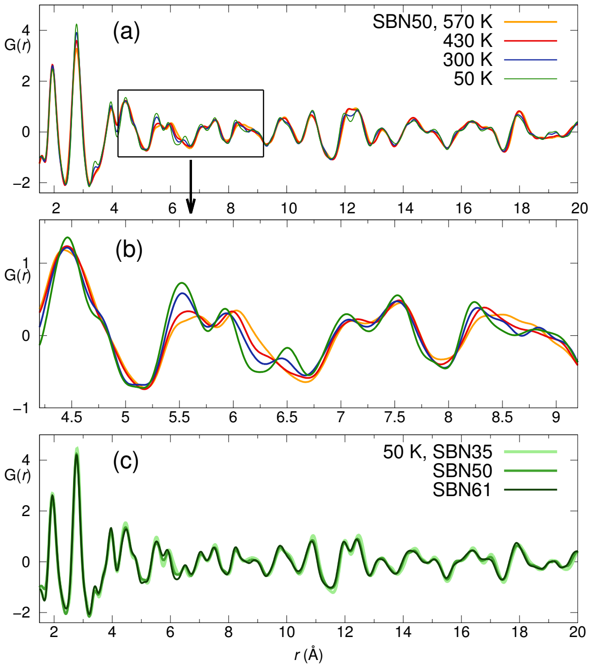

Figure 1: Neutron pair distribution function G(r) results of SBN100x. (a) Temperature dependence of G(r) for SBN50, (b) detail of $G(r)$ showing a range of distances with the most pronounced changes, (d) full G(r) of SBN35, SBN50 and SBN61 at 50 K.

2 Results

A selection of the collected data is presented in Fig. 1. The most pronounced temperature dependence is observed at distances $5.25 - 6.75$ Å and $8.25 - 9$ Å [enlarged in Fig. 1(b)] where the height of the peaks is reshuffled and an additional peak emerges at ∼6.5 Å on cooling. For SBN50 this peak appears at temperatures between $400 - 500$ K (see Fig. 2), while its

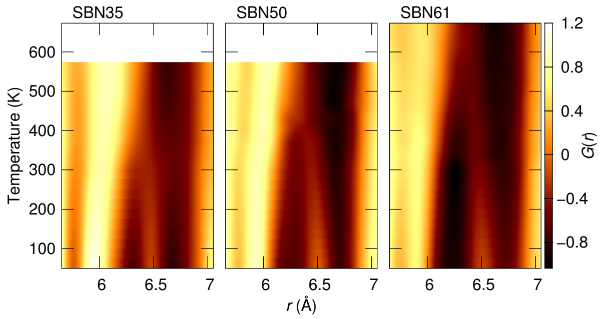

Figure 2: Temperature evolution of G(r) for SBN35, SBN50, and SBN61 powders. The interpolated maps show the influence of Sr content on the emergence of a peak at ~ 6.5 Å.

separation begins at higher temperatures for SBN61 and lower for SBN35 clearly implying Sr-content dependence. In Fig. 1(c) the $G(r)$'s for the three studied compositions at 50 K are compared showing that the difference between them is rather small.

The local structure of SBN is inevitably affected by the Sr/Ba occupational disorder as well as by the presence of vacancies. After testing existing models of SBN and making sure that none of them can satisfactorily explain observed PDF's, we turned to first principles (FP) calculations which allow for a model-free understanding of our data and facilitate a comprehensive analysis of the nanoscale structure.

In Fig. 3(a) we present a comparison of the experimental and calculated $G(r)$ profiles which, taking into account that no fitting was involved, display a remarkable agreement, especially in the previously discussed problematic range of distances ($5 - 9$ Å). PDF's obtained from *ab initio* molecular dynamics calculations [Fig. 3(b) and (c)] confirm that the same temperature-dependence is observed as in Figs. 1(b) and 2 with an emergence of the peak at ∼6.5 Å. Analysis of the FP structures revealed that the peak comes from tilting of oxygen octahedra. Clear dependence on Sr content is observed with the local tilting pattern starting to develop at higher temperatures for larger x (see Fig. 2).

Furthermore the attention was paid to the behaviour of Nb atoms with respect to the surrounding oxygen octahedra. Nb atoms are displaced from centers of octahedra at high temperatures and the distribution of displacement distances is preserved in the low-temperature structure (first PDF peak coming from Nb-O pairs is nearly temperature-independent). Different behavior on the two distinct crystallographic positions of Nb is observed from *ab initio* calculations with Nb(1) atoms shifting mostly along the tetragonal axis and Nb(2) atoms having large *ab*-plane components. Nb(1)O_6 chains are characterized by local polarization that freezes at high temperatures, well above the T_C. On the contrary, polarization of Nb(2)O_6 chains ceases to fluctuate at temperatures close to T_C. We argue that the *ab*-plane displacement disorder of Nb(2) atoms, interconnected with octahedra tilts and Sr displacements, is responsible for relaxor behaviour of Sr-rich SBN.

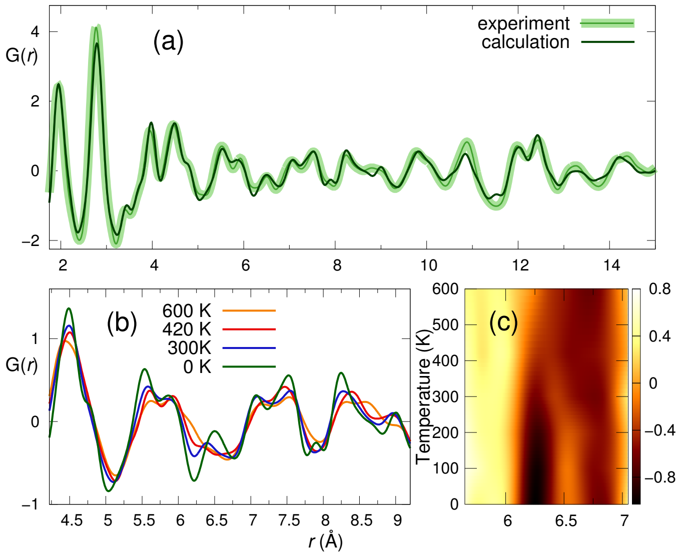

Figure 3: (a) Comparison of experimental (50 K) and calculated (0 K) PDF's for SBN50. The latter data has been corrected for the deviation from the experimental volume (1 %). No fitting procedure has been involved. (b) Temperature-dependent PDF from *ab initio* molecular dynamics calculations, for comparison with the data presented in Fig. 1(b). (c) An interpolated map for comparison with experiment in Fig. 2.

A comprehensive study based on this experiment and *ab initio* calculations is available on arXiv [2] and is under a minor revision anticipating publication in Physical Review B. It is a part of our undergoing research devoted to local-structural aspects of extraordinary electrooptical and dielectric properties of SBN [3].

References

[1] M. Pasciak, G. J. Cuello, H. E. Fischer, J. Hlinka, M. Kempa, J. Kulda, and P. Ondrejkovic, *Local structure of uniaxial ferroelectric relaxor (Sr,Ba)Nb2O6. Institut Laue-Langevin (ILL) doi:10.5291/ILL-DATA.6-06-463* (2015).

[2] M. Paściak, P. Ondrejkovic, P. Vanek, J. Drahokoupil, G. Steciuk, L. Palatinus, T. R. Welberry, J. Kulda, H. E. Fischer, J. Hlinka, et al., arXiv e-prints arXiv:1811.07823 (2018).

[3] M. Paściak, M. Kopecký, J. Kub, J. Fábry, J. Dec, P. Ondrejkovic, J. Hlinka, and E. Buixaderas, Phase Transitions **91**, 969 (2018).